

## Separation of Carbon Dioxide from Natural Gas through Matrimid-Based Mixed Matrix Membranes

Akbar Samadi<sup>1</sup>, Amir H. Navarchian<sup>2\*</sup>

<sup>1,2</sup>Chemical Engineering Department, Faculty of Engineering, University of Isfahan, Isfahan, Iran

### Article History

Received: 2017-03-03

Revised: 2017-05-25

Accepted: 2017-06-24

### Abstract

Spherical MgO nanoparticles and Flake-like clay minerals modified with polyaniline (PAni) are applied in Matrimid in order to fabricate mixed matrix membranes (MMMs) having improved gas separation performance. The CO<sub>2</sub> permeability, CO<sub>2</sub>/CH<sub>4</sub> selectivity and CO<sub>2</sub>-induced plasticization pressure of MMMs are assessed at 4-30 bar feed pressure. The chemical structure, morphology and thermal properties of MMMs are analyzed by Fourier transform infrared equipped with attenuated total reflection (FTIR-ATR), X-ray diffraction, field emission scanning electron microscopy (FESEM) and differential scanning calorimetry/thermogravimetric analyses. Crater-like morphology is seen for MMMs by FESEM tests. Physical interaction of Matrimid with MgO and PAni, confirmed by FTIR-ATR, helps better distribution of both the fillers in the polymer matrix. Mechanical analysis of gas sorption and diffusion terms reveals that PAni/clay (PC) enhances gas permeability by controlling diffusivity paths, while MgO nanoparticles improves both gas solubility and diffusivity. The permeability tests reveal that the sample PC5M5 with 5 wt% PC and 5 wt% MgO, has the best gas separation properties. High pressure tests reveal that this sample can enhance plasticization pressure and CO<sub>2</sub> permeability as well by 76% and 200%, respectively; resulting in 425% enhancement in MMMs capacity in natural gas sweetening.

### Keywords

CO<sub>2</sub> removal, mixed matrix membrane, matrimid, plasticization

### 1. Introduction

With respect to the expected growth in the demand for natural gas, it is necessary to upgrade low-quality natural gas by gas sweetening processes in order to decrease CO<sub>2</sub> and H<sub>2</sub>S content thereof (Hao, Rice, & Stern, 2002). In case of CO<sub>2</sub>, it causes corrosion in presence of any moisture and increases the cost of gas transportation (Colin A. Scholes, Stevens, & Kentish, 2012). In addition, the separation of CO<sub>2</sub> from industrial stack gases, is vital from the environmental point of view (Bhide, Voskericyan, & Stern, 1998). Nowadays, mixed matrix membranes (MMMs) are the subjects of many studies conducted in natural gas sweetening field because they combine the polymer advantages of processability, flexibility and availability with good separation property as well as the thermal/mechanical stability of inorganic fillers. Among many existing polymers studied in gas separations, the focus is

on polyimides due to their high gas permeability, high intrinsic permselectivity, appropriate mechanical strength and chemical stability as compared with other conventional membranes (Sridhar, Veerapur, Patil, Gudasi, & Aminabhavi, 2007). Matrimid® is a thermoplastic polyimide, widely applied as a commercial grade for gas separation processes (Tin et al., 2003). This polymer is plasticized by CO<sub>2</sub> at pressures around 10 bar at room temperature leading to an increase in permeabilities of all separating gases, thus, deterioration of selectivity. When the CO<sub>2</sub> concentration is high enough to interact with polymer chains, it can increase the segmental mobility and the free volumes within the macromolecules (Bos, Pünt, Strathmann, & Wessling, 2001). Plasticization can be suppressed by cross-linking, polymer blending and applying inorganic fillers in polymer matrix, that is, fabrication of MMMs (Dong, Li,

\* Corresponding Author.

Authors' Email Address:

<sup>1</sup>A. Samadi(akbar.samadi@ymail.com), <sup>2</sup>A. H. Navarchian(navarchian@eng.ui.ac.ir),

& Chen, 2011; Gh & Navarchian, 2016; Hosseini, Peng, & Chung, 2010; Hosseini, Teoh, & Chung, 2008; Ismail & Lorna, 2002; Perez, Balkus Jr, Ferraris, & Musselman, 2014; Shahid & Nijmeijer, 2014b; Su et al., 1997; Xiao, Low, Hosseini, Chung, & Paul, 2009). Various fillers like zeolites (Shahid & Nijmeijer, 2014a; Y. Zhang, Balkus Jr, Musselman, & Ferraris, 2008), silica (Ahn, Chung, Pinnau, & Guiver, 2008), alumina (Tena et al., 2010), clay (Bhole, Wanjale, Kharul, & Jog, 2007; Defontaine et al., 2010; Gh & Navarchian, 2016) and metal oxides (Hosseini, Li, Chung, & Liu, 2007) are applied in MMMs for gas separation. These fillers are appropriate candidates in overcoming the plasticization phenomenon and the permselectivity limitations of polymeric membranes for gas separation as presented by Robeson upper bound (Noble, 2011; Robeson, 2008). They may control the chain mobility by mutual interactions that prevent plasticization of polymer matrix at high feed pressures (Ismail & Lorna, 2002). The tortuosity of diffusion path increases by applying these fillers into the polymer matrix that improve the selectivity in the favor of smaller penetrant (Bertelle, Gupta, Roizard, Vallières, & Favre, 2006). This is due to the fact that the selectivity of polymers at temperatures below their glass transition temperature ( $T_g$ ) is mainly dominated by diffusivity term (Yampolskii, Pinnau, & Freeman 2006). While the fillers, may disrupt the polymer chain packing which leads to an increase in polymer free volume and generate voids in the polymer matrix that improve permeability of gaseous penetrants (Gh & Navarchian, 2016; Hashemifard, Ismail, & Matsuura, 2011; He, Pinnau, & Morisato, 2002; Liang et al., 2012). Several authors have assessed the effect of fillers on  $\text{CO}_2/\text{CH}_4$  separation behavior of MMMs. Hashemifard *et al.* reported significant increase in permeability of  $\text{CO}_2$  and  $\text{CH}_4$  by applying montmorillonite clays with different types of interlayer cations to the polyetherimide matrix (Hashemifard et al., 2011). Applying montmorillonite in polyethersulfone is reported by Liang et al (2012) to increase permeability values of both  $\text{CO}_2$  and  $\text{CH}_4$  gases. They attributed this improvement mainly to extra gas transport paths produced on the polymer-clay interface (Liang et al., 2012). Montmorillonite modified by polyaniline (PAni) was incorporated into Matrimid matrix, where, an enhanced permeability of  $\text{CO}_2$  and  $\text{CH}_4$  is observed as the small voids production in the polymer/clay interfaces (Gh & Navarchian,

2016). The plasticization pressure ( $P_{plast}$ ) is postponed to higher pressures when PC particles are applied.

Gas permeability in dense membrane is subject to solution-diffusion mechanism (Baker, 2004). Although, the selectivity of glassy polymers at temperatures below  $T_g$  is influenced mainly by the fillers with high aspect ratio like montmorillonite, that increase the diffusion path (Yampolskii et al., 2006), it is suggested that applying fillers with special functional groups, like magnesium oxide (MgO) nanoparticles with hydroxyl groups on the surface, can interact with polar gases including  $\text{CO}_2$  which would improve its solubility and gas permeability (Cong, Radosz, Towler, & Shen, 2007; Hosseini et al., 2007; Hu et al., 1997; Pacchioni, 1993). The polymer-particle interactions may reduce the chain mobility that results in less plasticization. It can be assumed, that applying these two kinds of fillers may enhance the permselectivity and plasticization behavior of dense membranes.

To the best of authors' knowledge, here, there exist no report suggesting simultaneous application of both modified silicate layer and MgO nanoparticles in the Matrimid matrix. In this study, two fillers with different geometry and chemical properties including flake-like PC and spherical MgO nanoparticles are applied in order to improve both permeability and selectivity of MMMs and their plasticization resistance in the  $\text{CO}_2/\text{CH}_4$  separation process. Chemical structure, morphology and thermal properties of fabricated membranes are analyzed through Fourier transform infrared equipped with attenuated total reflection (FTIR-ATR), X-ray diffraction (XRD), field emission scanning electron microscopy (FESEM), differential scanning calorimetry (DSC) and thermogravimetric analyses (TGA). The gas permeation tests are run at different pressures to evaluate permselectivity and plasticization behavior of MMMs. The effects of MgO and PC contents on the permselectivity and plasticization resistance of Matrimid membranes are assessed as well.

## 2. Methods and Materials

### 2.1. Materials

Matrimid<sup>®</sup>5218 (Hunstman LLC Corporation, Canada, CAS number 62928-02-6) and MgO nanoparticles (average size 1-5 nm, US NANO company, USA), are consumed preparation of MMMs. The TEM image of MgO nanoparticles is shown in Fig. (1-a). PC nanocomposite (Table 1) is consumed as synthesized by *in-situ*

polymerization of aniline in the presence of Cloisite 30B® (Gh & Navarchian, 2016). The solvent, N-methyl-2-pyrrolidone (NMP) is

purchased from Merck Company (Germany). The purchased chemicals are consumed upon receive.

**Table 1.** Characteristics of PAni/clay (PC) powder used in this study (Gh & Navarchian, 2016)

PAni specifications	Oxidation state: emeraldine base	
	Synthesized: <i>in-situ</i> polymerization in the presence of MMT through rapid mixing method.	
Polymerization yield: 62%		
PAni content <sup>a</sup>	80 wt%	
Clay specifications	Cloisite® 30B, an organo-modified montmorillonite containing alkyl ammonium ions purchased from Southern Clay Products (USA)	
Clay content <sup>a</sup>	20 wt%	
Surface area <sup>b</sup>	22.1 m <sup>2</sup> /g	
Total porosity <sup>b</sup>	0.15 cm <sup>3</sup> /g	
Average pore diameter <sup>b</sup>	6.94 nm	
Morphology <sup>c</sup>	Flower-petal PC morphology (long-chain PAni macromolecules synthesized inside the clay gallery spaces, forming PC flakes which are connected together while exfoliated)	

<sup>a</sup> measured through thermogravimetric analysis (TGA) under air atmosphere  
<sup>b</sup> measured by Brunauer–Emmett–Teller analysis  
<sup>c</sup> analyzed by scanning electron microscopy (Fig.. (1-b))

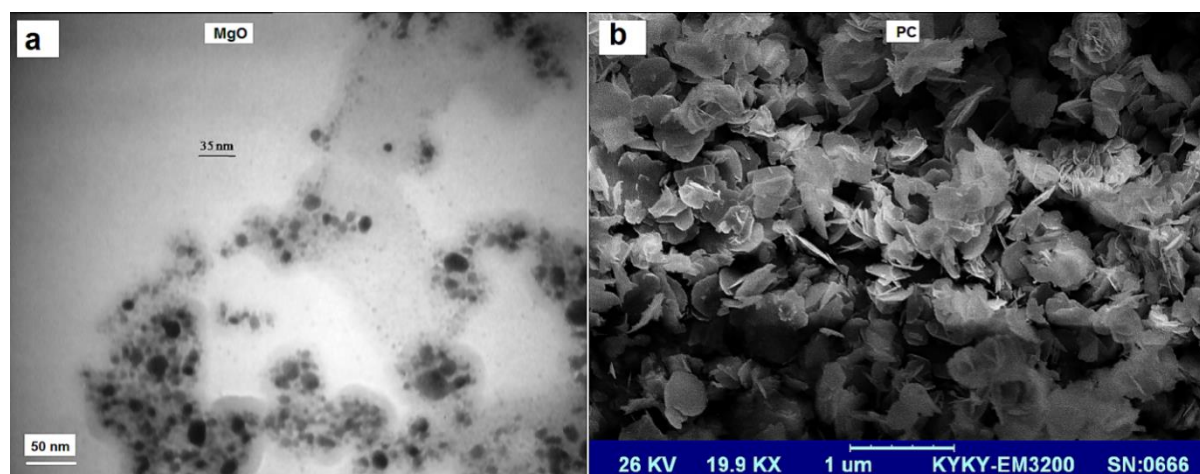


**Figure 1.** (a) TEM image of MgO nanoparticles prepared by the manufacturer, and (b) SEM image of PC powder (Gh & Navarchian, 2016).

## 2.2. Membrane Fabrication

Matrimid-based membranes containing different contents of MgO (0-10 wt%) and PC (0-10 wt%) fillers are fabricated through solution casting method (Hashemifard et al., 2011; Hosseini et al., 2007). The required volumes of Matrimid and MgO are dissolved in NMP by magnetic stirring and ultrasonication in a separate manner, next, the specified mass of PC is dispersed in NMP, stirred, ultrasonicated and then mixed with Matrimid/NMP and MgO/NMP solutions,

followed by further stirring, ultrasonication and filtration. The filtrate is casted in 8 cm-diameter Petri dishes and then dried completely in the oven at 120°C for sufficient time. Finally, the films are pilled from the glass and are dried at 200°C for 2-3 days to obtain membranes with the thickness of 60-70 microns. Fabricated samples are coded as PC<sub>x</sub>My, where, M is the MgO, and x and y are the PC and MgO weight percents, respectively, (e.g. PC<sub>5</sub>M<sub>5</sub> membrane contains 5 wt% of each fillers).

## 2.3 Membrane Characterization

There exist many techniques for characterization of fabricated MMMs

### 2.3.1 Fourier Transform Infrared

The chemical structure of fabricated membranes is analyzed through FTIR-ATR spectrophotometer (JASCO FT/IR-6300, Japan) equipped with attenuated total reflection (ATR) accessory at room temperature from 4000 to 400  $\text{cm}^{-1}$  with a spectral resolution of 4  $\text{cm}^{-1}$  and averaged over 32 scans.

### 2.3.2 X-Ray Diffraction

The microstructures of membranes are analyzed through XRD technique where a Bruker diffractometer (D8 ADVANCE, Germany) at the scan range of 5°-80° is applied.

### 2.3.3 Thermal Analysis

A simultaneous TGA/DSC system (STA 449F3 Jupiter, Netzsch, Germany) with a silicon carbide furnace is applied to assess the thermal properties of fabricated membranes. The samples of 5-10 mg weight are heated from 60 to 540°C at 10°C/min rate in the  $\text{N}_2$  atmosphere. The Netzsch Proteus Thermal Analysis software is applied for DSC and TGA data analysis.

### 2.3.4 Field Emission Scanning Electron Microscopy

FESEM (ZEISS SUPRA 35VP, Germany) is applied in analyzing the MMMs morphology. The samples are frozen and fractured in liquid nitrogen in order to monitor the membrane cross-section. The fractured samples are mounted on carbon tape masked on stainless steel stand and sputter-coated with 15 nm of gold prior to FESEM analysis.

## 2.4 Gas Permeability Tests

Gas permeability of all fabricated membranes are measured through a variable-pressure constant-volume apparatus (Model NM1390, Iran) by the following equation (Chung, Chan, Wang, Lu, & He, 2003):

$$P_A = \frac{273.15 \times 10^{10}}{760} \frac{LV}{AT(p_0)} \frac{dp}{dt} \quad (1)$$

where  $P_A$  is the permeability coefficient of the membrane to gas A in Barrer (1 Barrer =  $10^{-10} \text{ cm}^3(\text{STP}) \cdot \text{cm} / \text{cm}^2 \cdot \text{s} \cdot \text{cmHg}$ ),  $V$  is the volume of the downstream chamber ( $12 \text{ cm}^3 \pm 0.002 \text{ cm}^3$ ),  $A$  is the effective area of the film ( $17.1 \text{ cm}^2 \pm 0.0014 \text{ cm}^2$ ),  $L$  is the thickness of the membrane ( $0.007 \text{ cm} \pm 0.0001 \text{ cm}$ ),  $T$  is the

absolute temperature in measurement ( $298.15 \text{ K} \pm 0.1 \text{ K}$ ), and  $dp/dt$  is the pressure rate measured at downstream chamber (mbar/s) which is calculated in of 3 $\theta$  to 7 $\theta$  time range ( $\theta$  is the time lag in downstream pressure-time diagram) (Y. Zhang et al., 2008). The uncertainty pressure ( $p$  or  $p_0$ ) and time ( $t$ ) measurements is  $\pm 0.1$  mbar and  $\pm 0.1$  sec, respectively. The relative uncertainty of permeability of gas A ( $P_A$ ) is less than 1.6% based on Taylor equation (Taylor, 1997).

The ideal selectivity ( $\alpha$ ) of a membrane for gas A to gas B is assessed through the following equation:

$$\alpha = \frac{P_A}{P_B} = \frac{D_A \times S_A}{D_B \times S_B} = \frac{D_A}{D_B} \times \frac{S_A}{S_B} = \alpha_D \times \alpha_S \quad (2)$$

Where  $D$  ( $\text{cm}^2/\text{sec}$ ) and  $S$  ( $\text{cm}^3(\text{STP})/\text{cm}^3(\text{polymer}) \cdot \text{atm}$ ) are diffusivity and solubility of penetrants in the membrane matrix. Symbols  $\alpha_D$  and  $\alpha_S$  are the diffusivity-based and solubility-based selectivity values, respectively. The permeability tests are run at 4-10 bar and 25°C for all samples. The samples are examined at 4-30 bar pressure range to determine  $p_{plast}$  of MMMs and the effect of pressure on permeability and selectivity. The diffusion coefficient is obtained from the  $t$ -intercept,  $\theta$ , of the plot  $p$  against  $t$ , as suggested by Barrer (Crank, 1975; Taveira, Mendes, & Costa, 2003):

$$D = L^2 / 6\theta \quad (3)$$

The gas fluxes A ( $J_A$ ) ( $\text{cm}^3(\text{STP})/\text{cm}^2 \cdot \text{sec}$ ) through the membranes are calculated through the following equation (Baker, 2004):

$$J_A = P_A \cdot \Delta p_A / L \quad (4)$$

where,  $\Delta p_A$  is the pressure difference across the membrane.

## 3. Results and Discussion

### 3.1. Chemical Structure

Chemical structure of pristine Matrimid, PC0M5 and PC5M5 membranes, the PC powder and MgO nanoparticles are illustrated in Fig. (2). As observed in Fig. (2-c), the peaks at 1778  $\text{cm}^{-1}$  (C=O stretching of ketonic groups), 1716  $\text{cm}^{-1}$  (C=O anti-symmetric stretching of imide groups), 1669  $\text{cm}^{-1}$  (C=O stretching of imide groups), 1425  $\text{cm}^{-1}$  (bending vibrations of aliphatic C-H bonds), and 3484  $\text{cm}^{-1}$  (N-H bonds) constitute the characteristic peaks of Matrimid (Dong et al., 2011; Gh & Navarchian, 2016; Moghadam, Omidkhan, Vasheghani-Farahani, Pedram, & Dorosti,

2011; Pavia, Lampman, Kriz, & Vyvyan, 2015 ; Zhao et al., 2008). In the FTIR spectra of Matrimid-MgO and Matrimid-MgO-PC membranes and MgO nanoparticles, (Fig. (2-c\_)), the peak at 487-490  $\text{cm}^{-1}$  is attributed to the symmetric  $\text{Mg}=\text{O}$  bond (Figs 2 (b, d and e)). The FTIR spectrum of Matrimid-PC-MgO membrane is shown in (Fig. (2-c)). The peak at 1509  $\text{cm}^{-1}$  (stretching bonds of benzenoid rings) (Kang, Neoh, Tan, Khor, & Tan, 1990; Tang, Jing, Wang, & Wang, 1988) and the peak at 1377  $\text{cm}^{-1}$  (weak stretching of C-N bond in quinonoid-benzenoid-quinonoid (QBQ) successive units) (Cao, Li, Xue, & Guo, 1986) are the characteristic transmittance of emeraldine base PC powder which are also visible in FTIR spectrum of PC powder (Fig. (2-

a)) (Gh & Navarchian, 2016). The peaks of clay 30B at 400-600  $\text{cm}^{-1}$  (ascribed to Si-O bending and Al-O stretching), and 1035  $\text{cm}^{-1}$  (attributed to Si-O stretching) are observed in FTIR spectra of PC powder (Fig. (2-a)) and Matrimid-PC-MgO membrane (Kataria, 2005). Some shifts in Matrimid appearance peaks (the peak at 1294  $\text{cm}^{-1}$  for bending of C-CO-C groups) and PC (the C-H stretching at 1302  $\text{cm}^{-1}$  and stretching bonds of quinonoid rings at 1587  $\text{cm}^{-1}$ ) may indicate the possible compatibility of these two polymers because of hydrogen bonding between carbonyl groups of Matrimid and N-H group in secondary amine functional groups of PANi (Jiang, Wang, Chung, Qiao, & Lai, 2009).

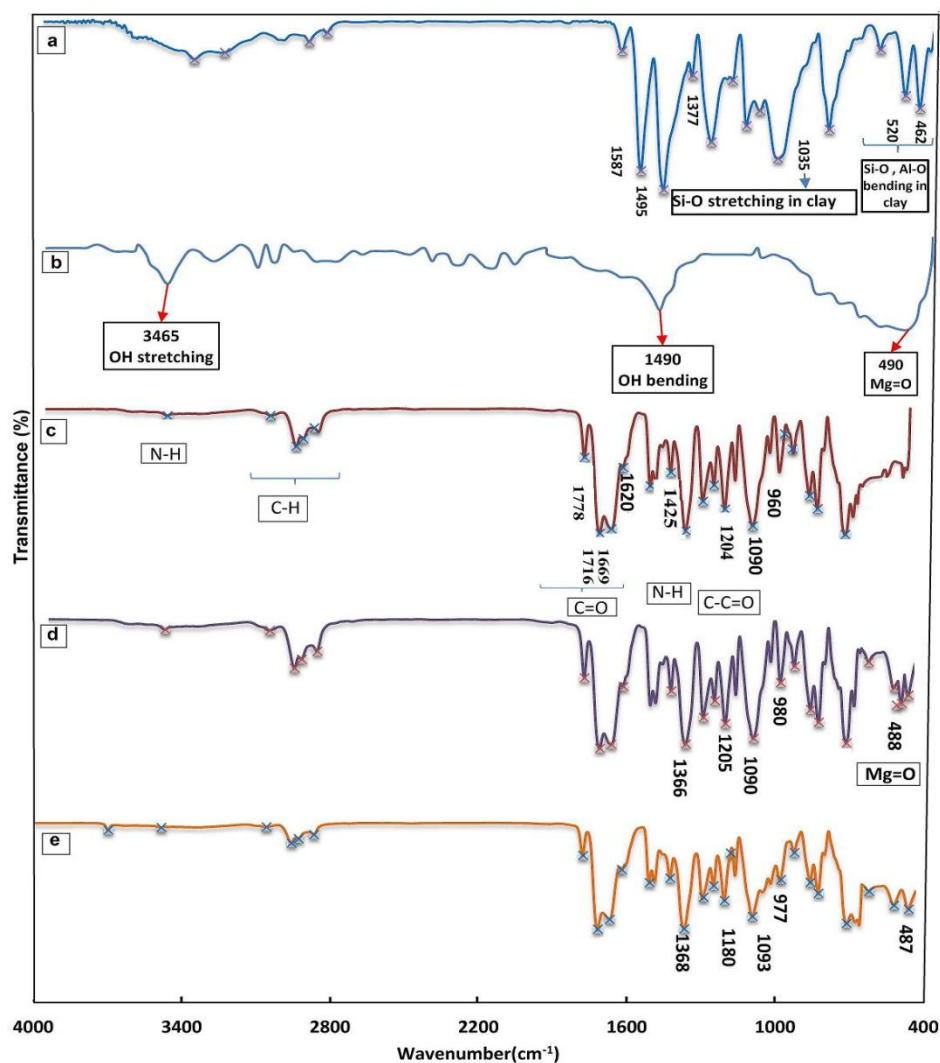


**Figure 2.** FTIR spectra of (a) PC powder, (b) MgO nanoparticles, (c) Matrimid membrane, (d) PC0M5 and (e) PC5M5.

### 3.2 Microstructure

The X-ray spectra of Matrimid membrane and corresponding MMMs are shown in Fig. (3). A broad peak observed at  $2\theta$  about  $20^\circ$  indicates the amorphous nature of Matrimid (Ebadi Amooghini, Omidkhan, & Kargari, 2015; Hosseini et al., 2007; Sridhar et al., 2007). Presence of this peak is often interpreted as a measure of the average intersegmental distance between the polymer chains (Aziz & Ismail, 2010; Ghosal & Freeman, 1994). Appearance of the same peak with the same broadness and strength in the XRD spectra of MMMs reveals that the incorporation of the neither of fillers in general alter the microstructure of the Matrimid matrix. As observed in Fig. (3), there exists no sharp peak representing the peaks of MgO nanoparticles. As declared by Hosseini et al. (Hosseini et al., 2007), this is attributed to the low concentration of MgO in membrane matrix.

### 3.3 Thermal Properties

The DSC/TGA graphs of Matrimid-PC (sample PC5M0) and Matrimid-PC-MgO (sample PC5M5) membranes are shown in Fig. (4), where all endothermic peaks shown in DSC curves of the samples below  $150^\circ\text{C}$  are attributed to the evaporation of trace amount of volatile compounds including water, HCl,  $\text{NH}_4\text{OH}$ , etc. with a weight loss less than 1% as seen in TGA curves (Gh & Navarchian, 2016; Narayanan et al., 2010). For both membranes, the weight loss from  $150^\circ\text{C}$  to  $200^\circ\text{C}$  (1-2%) is mainly due to the evaporation of NMP (boiling point:  $202$  to  $204^\circ\text{C}$  (Rajiv Mahajan, Burns, Schaeffer, & Koros, 2002)). The extra weight loss of about 8% at  $200$ - $455^\circ\text{C}$  (for sample PC5M0) and  $200$ - $473^\circ\text{C}$  (for sample PC5M5) ranges with an endothermic peak at  $280$ - $290^\circ\text{C}$  is probably attributed to the loss of organic cation of 30B clay, evaporation and/or decomposition of low molecular weight PANi

oligomers of the PC particles (Anadão, Sato, Wiebeck, & Valenzuela-Díaz, 2010; Ansari, Yadav, Cho, & Mohammad, 2013). An exothermic peak at  $495$ - $496^\circ\text{C}$  is attributed to the thermal decomposition of PC and Matrimid observed in both samples. The onset of thermal decomposition of PC5M0 and PC5M5 are  $455^\circ\text{C}$  and  $473^\circ\text{C}$  which is higher than that of neat Matrimid ( $410^\circ\text{C}$ ), reported by (Perez et al., 2014). This represents an enhanced thermal stability of the membranes by incorporating PC (Anadão et al., 2010; Shi & Gan, 2007) and MgO (Moaddeb & Koros, 1997). The dispersed clay platelets probably act as barriers caused by labyrinth effect (tortuous path) (Lu, Hu, Li, Chen, & Fan, 2006) for both heat and mass transfer (Anadão et al., 2010). As for MgO, it is assumed that high stiffness MgO nanoparticles may hinder long-range mobility of polymer chains which increase thermal stability of the polymer (Moaddeb & Koros, 1997). This phenomenon can be verified by analyzing the glass transition temperature ( $T_g$ ) of the samples. As observed in Fig 4, the  $T_g$  of PC5M0 is about  $310^\circ\text{C}$ , corresponding to that of the Matrimid  $T_g$ . The  $T_g$  of PC5M5 is enhanced at  $335^\circ\text{C}$  where the stiffness of the polymer is enhanced by applying MgO nanoparticles.

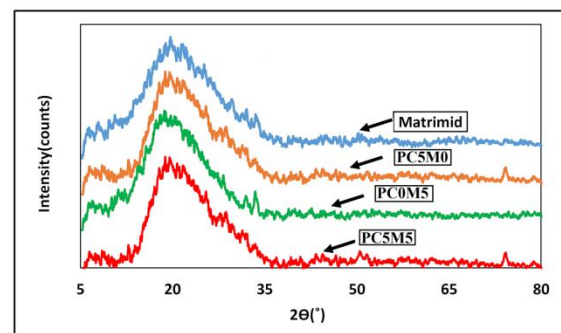


**Figure 3.** XRD patterns of pristine Matrimid, PC0M5, PC5M0 and PC5M5 membranes, in the range of  $5^\circ$ - $80^\circ$ .

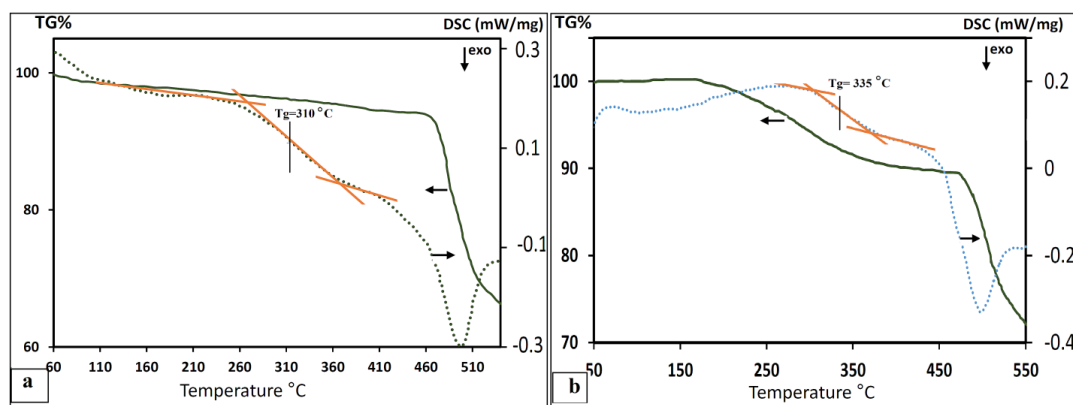


**Figure 4.** TGA (solid lines) and DSC (dashed lines) thermographs of samples PC5M0 (a) and PC5M5 (b).

### 3.4 Morphology

The FESEM images of MMMs are shown in Fig. (5), where in sections 5(a, b and c), there is no significant accumulation of MgO or PC particles on the membrane surface. This is due to the appropriate of concentration (and, viscosity) and temperature of casting solution rates (Aroon, Ismail, Matsuura, & Montazer-Rahmati, 2010; R. Mahajan, 2000).

As observed in Figs 5 (d, e and f), the cross-sections of MMMs have a crater-type morphology (Ge, Zhou, Rudolph, & Zhu, 2013; Gh & Navarchian, 2016; Shahid & Nijmeijer, 2014b). The creation of elongated matrix around the crater edges is probably because of the interfacial stress concentrations between polymer and fillers (Y. Zhang et al., 2008). Several authors suggest similar morphology for different kinds of nanosized fillers like metal-organic frameworks (MOFs) (Dorosti, Omidkhah, & Abedini, 2014; Ge et al., 2013; Shahid & Nijmeijer, 2014a, 2014b) and ordered mesoporous silica spheres (Khan, Klaysom, Gahlaut, Khan, & Vankelecom, 2013) in various polymer matrices including polyimides. A different morphology is observed, for MMMs containing a micron-size MOF (Ploegmakers, Japip, & Nijmeijer, 2013), Probably indicating that the filler size plays a more important than the chemical/physical nature of components in formation of this morphology.

Here, the presence of particles smaller than  $0.1 \mu$  in the center of the craters is probably due to some minor aggregation of MgO particles not present in PC5M0. As to similar particle size in these two membranes, it is assumed that addition of both 5 wt% PC and 5 wt% MgO do not lead to particles' interference, thus, more agglomeration. This is most probably because of difference in the nature of chemical and physical properties of the two fillers. It is assumed that PANi acts as a sizing agent on clay minerals and prohibits their interaction with MgO nanoparticles (Aroon et al., 2010). This can assist the successful incorporation of the fillers at relatively high concentrations in improving the Matrimid gas separation properties.

A few pores are observed in the membranes cross sections. Because these pores are not observed in the FESEM images of the membrane surfaces (Figs (5-a, b and c)), it is assumed that they are not formed along the gas permeation direction and do not make short-cut paths for gas molecules, thus, keeping sufficient gas selectivity for the membrane. The unconnected-pores in the cross section of the membranes are mainly the result of the residual stresses imposed during solvent evaporation and depend on volume of solvent left to be removed when the nascent polymer matrix is vitrified (Moore & Koros, 2005)

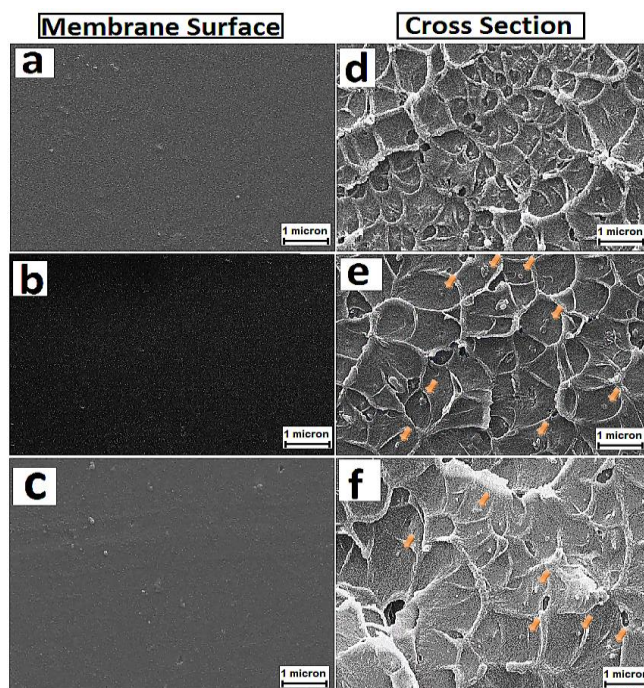


**Figure 5.** FESEM images of PC5M0 (a and d), PC0M5 (b and e) and PC5M5 (c and f). The left and right photos indicate the membranes surface and cross-section, respectively. Magnifications of all images are 20 kX. (The arrows illustrate MgO agglomerates)

### 3.5 Permeability and Selectivity of Membranes

#### 3.5.1 Matrimid-MgO Membranes

The images of permeability and selectivity of Matrimid-based membranes containing 0-10 % (wt.) MgO are illustrated in Figs 6 (a, b and c). Permeabilities of CO<sub>2</sub> and CH<sub>4</sub> in pristine Matrimid membrane at 4 bar feed pressure are 7.8 and 0.26 Barrer, respectively, and both increase to about 14 and 0.5 Barrer, respectively, together with increasing MgO concentration to 10%. This phenomenon can probably be attributed to the fact that MgO nanoparticles interaction with Matrimid macromolecules, leading to chain packing within the polymer chains, an increase in their free volume and enhance gas permeabilities (Matteucci, Kusuma, Kelman, & Freeman, 2008). The fact that the CO<sub>2</sub>/CH<sub>4</sub> selectivity is kept high at 28-38 range for various MgO contents and different pressures is expressed in Fig. (6-b). Smaller dynamic molecular diameter and higher condensability of CO<sub>2</sub> molecules in comparison with those of CH<sub>4</sub> lead to higher

diffusion and solubility coefficients of this gas, ending in relatively high CO<sub>2</sub>/CH<sub>4</sub> selectivity values (Chung et al., 2003; Colin A Scholes, Tao, Stevens, & Kentish, 2010). As observed in Fig (6-c), the CO<sub>2</sub>/CH<sub>4</sub>selectivity is enhanced gradually by applying up to 5 % MgO and then a slight fall. This can be explained by two contradicting effects of MgO nanoparticles on CO<sub>2</sub>/CH<sub>4</sub> selectivity. MgO has basic property and may have specific interactions with acidic CO<sub>2</sub> leading to an increase in CO<sub>2</sub>/CH<sub>4</sub>selectivity at a specified MgO content (Mekhmer, Halawy, Mohamed, & Zaki, 2004). At higher MgO contents, excess free volume and generated voids together with possible agglomeration of particles, deteriorate the CO<sub>2</sub>/CH<sub>4</sub> selectivity (Perez et al., 2014). The sample with 5% MgO (sample PC0M5) is of the best performance among the examined samples, because the CO<sub>2</sub> permeability increases up to 35-40% and CO<sub>2</sub>/CH<sub>4</sub> selectivity enhances by 3±0.3 units as compared with that of Matrimid membrane at the test pressures of 4-10 bar, Figs 6(a, b and c).

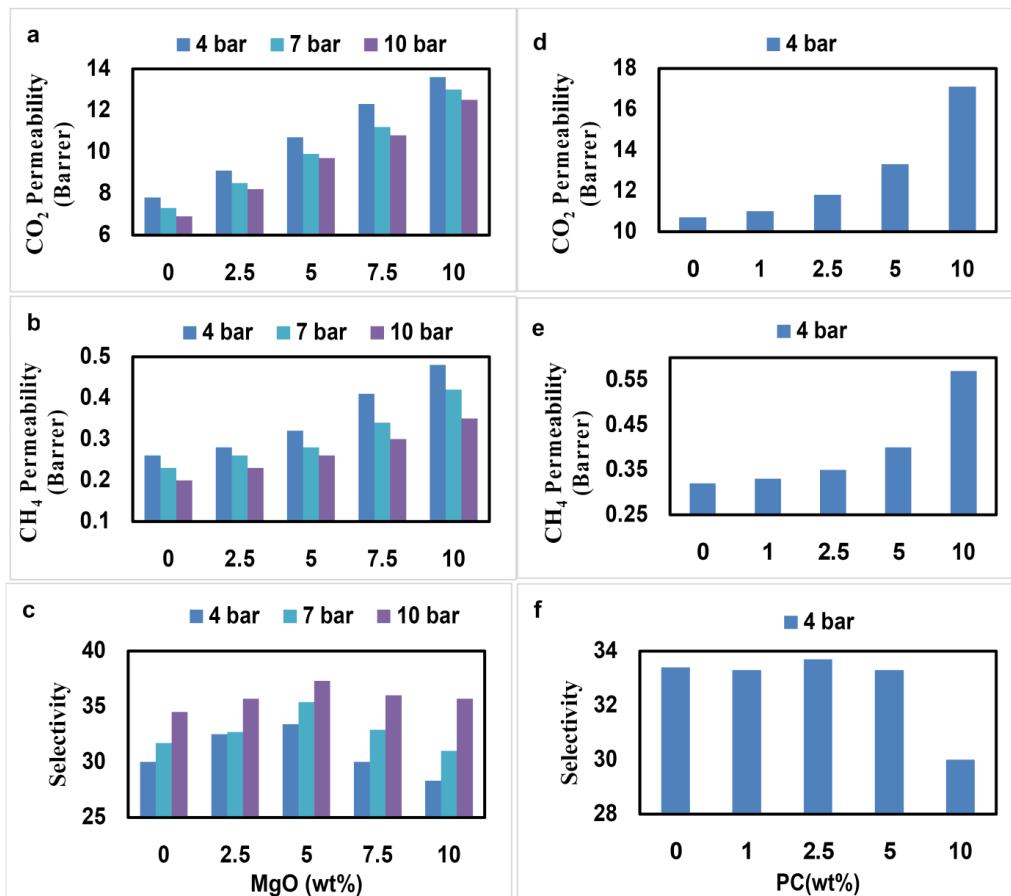


**Figure 6.** Effect of MgO content on (a) permeability of CO<sub>2</sub>, (b) permeability of CH<sub>4</sub> and (c) selectivity of CO<sub>2</sub>/CH<sub>4</sub> for Matrimid-based membranes at 4-10 bar and 298 K. Effect of PC content on (d) permeability of CO<sub>2</sub>, (e) permeability of CH<sub>4</sub> and (f) selectivity of CO<sub>2</sub>/CH<sub>4</sub> for Matrimid-MgO (5 wt%) membranes at 4 bar and 298 K. Relative uncertainties are less than 1.6% and 3.2% for permeability and selectivity, respectively.

The permeability of Matrimid-MgO membranes for both gases decreases subject to an increase in pressure from 4 to 10 bar. The permeability of gas through a dense membrane is a product of its solubility and diffusivity coefficients (Baker, 2004):

$$P = S \times D \quad (5)$$

The gas sorption capacity is defined Eq.(6) (Yampolskii et al., 2006):

$$C = S \times p \quad (6)$$

where,  $S$  is the solubility coefficient and  $p$  is the gas pressure. The three-parameter dual-mode sorption isotherm model can describe gas sorption in glassy polymers (Paul, 1979):

$$C = K_d p + C'_H \frac{bp}{1 + bp} \quad (7)$$

where,  $K_d$  is the Henry's law parameter,  $C'_H$  is the Langmuir sorption capacity, and  $b$  is the Langmuir affinity parameter. The solubility coefficient is calculated through Eqs. (6 and 7):

$$S = \frac{C}{p} = K_d + C'_H \frac{b}{1 + bp} \quad (8)$$

The solubility decreases subject to pressure, and approaches to the Henry's law parameter at very high pressures. In glassy polymers, the diffusion coefficient for a gaseous penetrant increases slowly at relatively low pressures. This behavior corresponds to the transport model based on dual-mode concepts (Koros, Paul, & Rocha, 1976). The solubility and diffusion coefficient correlation with pressure determines, the permeability pressure behavior. Since the former is dominant, the dual-mode sorption and the mobility models predict a decrease in permeability with an increase in pressure which is mainly due to the lower solubility of gases at higher pressure (Bos, Pünt, Wessling, & Strathmann, 1998; Duthie et al., 2007; Ismail & Lorna, 2002; Wind, Staudt-Bickel, Paul, & Koros, 2002; L. Zhang, Xiao, Chung, & Jiang, 2010).

The effect of MgO content and pressure on the gas permselectivity of membranes, can be analyzed by computing the gas sorption properties of a mixed-matrix membrane based on the additive model as follows (Barrer, Barrie, & Rogers, 1963; Matteucci, Kusuma, Sanders, Swinnea, & Freeman, 2008):

$$C_{MMM} = [(\sum (\phi_F C_F) + (1 - \sum \phi_F) C_{polymer})](1 - \phi_V) + \phi_V C_V \quad (9)$$

Where  $C_{MMM}$ ,  $C_F$  and  $C_{polymer}$  are the gas concentration (the amount of adsorbed gas per volume) in the nanocomposite (MMM), the filler and the polymer ( $\text{cm}^3(\text{STP})/\text{cm}^3$ ),

respectively.  $C_V$  is the gas concentration in the polymer/particle interfacial voids, obtained by the ideal gas law for a given pressure ( $p$ ) and temperature ( $T$ ):

$$C_V = \frac{p}{RT} \quad (10)$$

Gas concentration in a void is, obtained as being  $0.88 \text{ cm}^3(\text{STP})/(\text{cm}^3 \text{ void})$  at standard conditions.

In Equation 9,  $\phi_V$  is the void volume percentage and  $\phi_F$  is the volume percentage of filler, that is:

$$\phi_F = \frac{\omega_F / \rho_F}{\omega_F / \rho_F + \omega_P / \rho_P} \quad (11)$$

where,  $\rho_F$  and  $\rho_P$  are the density of filler and polymer, and  $\omega_F$  and  $\omega_P$  are the filler weight and polymer, respectively.

Gas sorption capacity of filler (MgO) is described as a function of pressure by the Freundlich isotherm (Matteucci, Raharjo, Kusuma, Swinnea, & Freeman, 2008):

$$C_F = K p^{1/n} \quad (12)$$

where,  $K$  and  $n$  are the fitting parameters as reported by Matteucci (Table 2) (Matteucci, Kusuma, Kelman, et al., 2008). As discussed, MgO indicate a greater sorption capacity for  $\text{CO}_2$ , due to acid-base interaction. Substitution of gas concentration values with each one of the MMM component (from equations 7, 10 and 12) in Equation 9, yields:

$$C_{MMM} = \left[ \begin{array}{l} \phi_{MgO} K p^{1/n} + (1 - \phi_{MgO}) \\ (K_d p + C'_H \frac{bp}{1 + bp}) \end{array} \right] \quad (13)$$

$$(1 - \phi_V) + \phi_V \frac{p}{RT}$$

The last term (void contribution on gas uptake) in Eq. (13) is neglected when compared with filler and polymer contributions (Matteucci, Kusuma, Kelman, et al., 2008), thus:

$$C_{MMM} = \left[ \begin{array}{l} \phi_{MgO} K p^{1/n} + (1 - \phi_{MgO}) \\ (K_d p + C'_H \frac{bp}{1 + bp}) \end{array} \right] \quad (14)$$

Here, the gas sorption capacity of MMMs can be assessed at any pressure and filler concentration. For this purpose, first, diffusion coefficients of both gas types in Matrimid membrane at different pressures are calculated by the time lag experimental method (Equation 3). The gas sorption data of pristine Matrimid are then obtained from permeability data through Eq.s (5 and 6) and finally, the dual-sorption parameters ( $K_d$ ,  $C'_H$ , and  $b$ ) of Matrimid are extracted by fitting Eq. (7) according to Table 2.

In the next step, the effect of MgO nanoparticles on gas sorption properties of MMMs at two different pressures (1 and 4 bar) are calculated through Eq. (14), Table 3, where, the concentration of gaseous penetrants on the MMMs ( $C_{MMM}$ ) is higher than that of neat Matrimid ( $C_{polymer}$ ), thus the reason for enhanced permselectivity of MMMs when MgO nanoparticles are applied.

**Table 2.** Freundlich isotherm parameters for gas adsorption onto MgO (Matteucci, Kusuma, Swinnea, & Freeman, 2008) and dual-mode sorption parameters of pristine Matrimid at 25 °C

	MgO Freundlich isotherm parameters		Matrimid dual-mode sorption parameters		
	$K$ ( $\text{cm}^3(\text{STP})/(\text{cm}^3 \text{MgO} \cdot \text{atm}^{1/n})$ )	$n$	$K_d$ ( $\text{cm}^3 \text{STP}/(\text{atm} \cdot \text{cm}^3 \text{polymer})$ )	$C'H$ ( $\text{cm}^3 \text{STP}/(\text{atm} \cdot \text{cm}^3 \text{polymer})$ )	$b$ ( $\text{atm}^{-1}$ )
CH <sub>4</sub>	50±8	2.5±0.2	0.4	5.4	0.2
CO <sub>2</sub>	63±10	3.2±0.2	1.2	14.6	0.5

**Table 3.** Gas sorption data ( $\text{cm}^3$  gas in STP/ $\text{cm}^3$ ) of MgO, Matrimid and MMMs at two different pressures (1 and 4 bar)

Pressure (bar)	Gas	$C_F$	$C_{polymer}$	$C_{PC0M5}$	$C_{PC0M10}$
1	CH <sub>4</sub>	50	1.3	3.8	6.2
1	CO <sub>2</sub>	63	6.1	8.9	11.8
4	CH <sub>4</sub>	87	4.0	8.1	12.3
4	CO <sub>2</sub>	97	14.5	18.7	22.8

### 3.5.2 Matrimid-MgO-PC membranes

Permeability and selectivity of Matrimid-MgO-PC membranes (PCxM5) with 5 wt% MgO and different PC loadings are illustrated in Figs 6 (d, e and f) for a typical feed pressure (4 bar). These samples are analyzed in order to assess the incorporation effect of two kinds of fillers on the gas separation properties of Matrimid membranes it is observed that applying PC particles enhances the membrane permeability in both gases types. As observed in Table 1, PC powder is comprised of 80 wt% emeraldine-base PAni. Rebattet and et. al (Rebattet, Escoubes, Pinéri, & Geniès, 1995) have already suggested that the sorption capacities of CO<sub>2</sub> and CH<sub>4</sub> on emeraldine-base PAni at 1 bar pressure are 4 and 1.5  $\text{cm}^3$  in STP/ $\text{cm}^3$  polymer, respectively. These values are almost in the same order of Matrimid gas sorption capacity reported in Table 3 and also those mentioned in other references (Chung et al.,

2003; Moghadam et al., 2011). It is suggested that any possible interaction between penetrating gas types with silicate layers (e.g. Si-OH) do not affect the solubility of CO<sub>2</sub> or CH<sub>4</sub> on the membranes (Ahn et al., 2008; Anadão et al., 2010; Bhole et al., 2007; Defontaine et al., 2010; Hashemifard et al., 2011; Liang et al., 2012). Thus, the PAni/clay (PC) particles do not probably make any significant change in gas sorption properties of fabricated membranes and the enhanced membrane permeability for both gas types at higher PC content is probably mostly attributed to the diffusion term. The SEM analysis of PC indicate a flower-petal like morphology of about 7 nm average pore size (Gh & Navarchian, 2016). The effect of the generated voids at polymer-filler interface is discussed for mixed-matrix membranes by Mahajan. It is found that presence of nonselective permeable regions in the polymer-filler interphase, results in selectivity of MMMs to drop to the selectivity of pristine polymer membrane level (R. Mahajan, 2000). Consequently, due to contradicting effects of tortuosity and void formation on diffusivity of gaseous penetrants, the CO<sub>2</sub>/CH<sub>4</sub> selectivity remains almost unchanged upto 5% PC content and then drops when the PC loading is increased to 10 wt% (Fig. (6-f)). A close examination of Fig. (6), indicates that the sample PC5M5 is assumed to have the best performance among the examined samples because its CO<sub>2</sub>/CH<sub>4</sub> selectivity is enhanced by 3.3 units (by MgO nanoparticles), and its permeability for CO<sub>2</sub> is increased by 70 % (due to presence of PC) compared to pristine Matrimid membrane. Comparing pristine membrane with three MMMs, each containing totally 10 wt% filler (samples PC5M5, PC0M10 and PC10M0), confirms that the sample PC5M5 has the best permselectivity performance on the Robeson chart (Fig. (7)). This can be verified by FESEM analysis that represents the same distribution of the fillers in sample PC5M5 with samples PC0M5 and PC5M0. This finding declares that incorporation of two kinds of fillers at lower concentrations (5 wt% PC and 5 wt% MgO) resulted in less agglomeration when compared with the membrane with only one type of filler at higher concentration (10 wt% PC or 10 wt% MgO). Here, it can be deduced that the applying PC and MgO with different geometry and physicochemical properties enhance Matrimid permeability and selectivity in CO<sub>2</sub> from CH<sub>4</sub> separation.

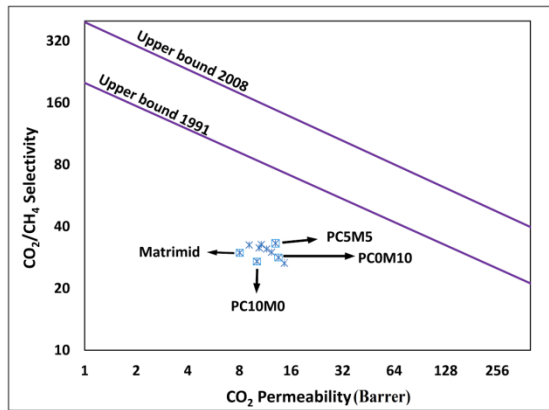


**Figure 7.** The comparison of permselectivity results of fabricated Matrimid and corresponding MMMs in Robeson chart. All symbols are related to different MgO and/or PC contents. (data for PC10M0 are adopted from our previous work (Gh & Navarchian, 2016)).

### 3.6 Effect of fillers on plasticization resistance of the MMMs

The effect of MgO content on plasticization resistance is analyzed. As pressure increases, Matrimid is plasticized by CO<sub>2</sub> at 10 bar pressure at room temperature (Bos et al., 2001; Bos et al., 1998; Bos, Pünt, Wessling, & Strathmann, 1999). As observed in Fig. (8-a),  $p_{plast}$  of the Matrimid-based membrane containing only MgO (without any PC) is increased slightly from 10 bar to 15 bar as the MgO content in the polymer is increases from zero (in pristine Matrimid) to 10 wt%. The reported maximum  $p_{plast}$  of Matrimid/nanofiller systems is up to 21 bar in Matrimid/MOF system (Shahid & Nijmeijer, 2014b). Matrimid-PC membranes (without MgO) have  $p_{plast}$  of 30 bar as found in our previous work (Gh & Navarchian, 2016). In other Matrimid-based

systems the plasticization has been postponed to 30-40 bar by thermal treatment (Bos et al., 1998), crosslinking (Tin et al., 2003) or polymer blending (Khan, Li, & Vankelecom, 2011) while the permeability and/or selectivity parameters faced significant deterioration.

$p_{plast}$  of Matrimid-PC membranes containing 5 wt% MgO (PCxM5)- (Fig. (8-d)) is slightly higher than that of Matrimid-PC membranes (MgO-free) with the same PC content (PCxM0), Table 4. It is suggested that the improvement of  $p_{plast}$  is mainly the result of introducing high modulus rigid silicate layers (Joulazadeh & Navarchian, 2010, 2011) which can entangle with Matrimid matrix and increase the chain stiffness (Ismail & Lorna, 2002), applying high plasticization resistant PAni (Gupta, Hellgardt, & Wakeman, 2006). MgO nanoparticles may hinder intrasegmental mobility of polymer backbone and so suppress plasticization (Ismail & Lorna, 2002).

Because of the plasticization phenomena in the glassy polymers, their gas separation capacity is limited, while one of the important characteristics of a membrane is its operating pressure. The fluxes of treated CO<sub>2</sub> in fabricated MMMs (calculated by Equation 4) indicate that by applying 5% PC and 5% MgO in Matrimid, CO<sub>2</sub> permeability and  $p_{plast}$  improve by 76% and 200%, respectively, while the selectivity is almost unchanged. For this membrane, the membrane capacity (the flux of the treated CO<sub>2</sub> through the membrane) can be obtained as  $46.8 \times 10^{-5} \text{ cm}^3(\text{STP})/\text{cm}^2$ , Eq. (4), where it is 425% when compared to the flux of CO<sub>2</sub> through the pristine membrane in natural gas processing at  $p_{plast}$  (30 bar) with the selectivity of 39.7, Table 4.

**Table 4.** Permeability, selectivity, and flux of CO<sub>2</sub> permeate through fabricated MMMs at  $p_{plast}$ . Data for Matrimid-PC membranes (PCxM0) are adopted from our previous work (Gh & Navarchian, 2016).

Membrane	$p_{plast}$ (bar)	$P_{CO_2}$ at $p_{plast}$ (Barrer)	$\alpha_{CH_4}^{CO_2}$ at $p_{plast}$	$J_{CO_2}$ at $p_{plast}$ $\text{cm}^3(\text{STP})/\text{cm}^2.\text{sec}$
PCOM0 (Matrimid)	10	7.0	40.0	$8.9 \times 10^{-5}$
PCOM5	15	9.2	36.8	$17.5 \times 10^{-5}$
PC1M0	15	-	-	-
PC1M5	15	9.2	35.4	$13.9 \times 10^{-5}$
PC2.5M0	20	-	-	-
PC2.5M5	20	10.1	38.8	$25.6 \times 10^{-5}$
PC5M0	25	-	-	-
PC5M5	30	12.3	39.7	$46.8 \times 10^{-5}$
PC10M0	30	-	-	-
PC10M5	30	13.6	37.8	$51.9 \times 10^{-5}$

### 3.7 Effect of Pressure on Selectivity of the MMMs

Permeability of CH<sub>4</sub> at PCOMx (Fig. (8-b)) and PCxM5 samples (Fig. (8-e)), at 4-30 bar gas pressure are measured to determine the effect of pressure on CO<sub>2</sub>/CH<sub>4</sub> selectivity as illustrated in Figs 8(c and f). It is observed that the selectivity increases with pressure upto 10-12 bar, then remains almost constant at higher pressures. The same behavior is observed in Matrimid-PC samples without any MgO (Gh & Navarchian, 2016). Selectivity is composed of two terms,  $\alpha_D$  and  $\alpha_S$  Eq. (2); the former is the

most dominant factor in the selectivity of glassy polymers (Yampolskii et al., 2006) and is a function of penetrant concentration in the polymer matrix (Ghosal & Freeman, 1994; Koros et al., 1976). As CO<sub>2</sub> is more condensable and diffusive than CH<sub>4</sub>, its concentration in polymer matrix is higher than that of CH<sub>4</sub>. At low pressures, concentration of CO<sub>2</sub> is just high enough in the polymer matrix to increase its diffusion coefficient, thus, the selectivity increase with pressure. An increase in pressure increases both, the CH<sub>4</sub> concentration in the polymer and its diffusivity, which lead to a constant selectivity at higher pressure.

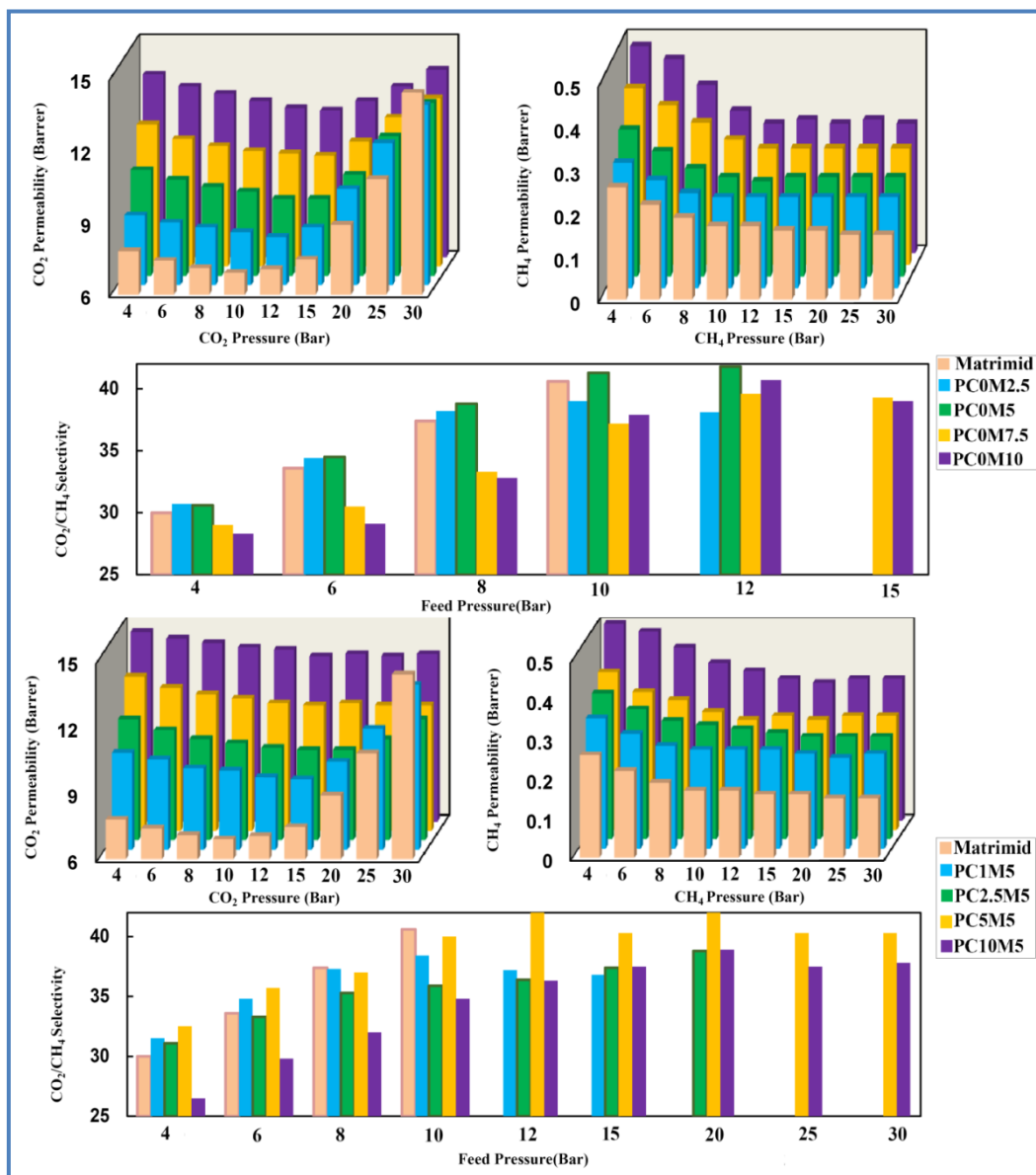


**Figure 8.** Effect of pressure on permeability of (a) CO<sub>2</sub>, (b) CH<sub>4</sub> and (c) selectivity of CO<sub>2</sub>/CH<sub>4</sub> for Matrimid membranes with different MgO content at 298 K. Effect of pressure on permeability of (d) CO<sub>2</sub>, (e) CH<sub>4</sub> and (f) selectivity of CO<sub>2</sub>/CH<sub>4</sub> for Matrimid-MgO (5 wt%) membranes with different PC content at 298 K. Relative uncertainties are less than 1.6% and 3.2% for permeability and selectivity, respectively.

#### 4. Conclusions

The focus of this study is on effective application of two types of fillers (MgO nanoparticle and PC nanocomposite) with different size and geometry into Matrimid-based MMMs. The generated MMMs indicated an enhancement in both permeability and selectivity in comparison with Matrimid for separation of CO<sub>2</sub> from natural gas. A crater type morphology is observed for MMMs as a characteristics of Matrimid-based membranes. It is found that PC only enhances gas permeability by the control of diffusivity paths, while MgO nanoparticles enhance both gas solubility and diffusivity. The obtained results indicate that sample PC5M5 containing both fillers at lower concentration (5 wt% PC and 5 wt% MgO) has the best gas separation properties. High pressure tests revealed that sample PC5M5 can enhance  $p_{plast}$  and CO<sub>2</sub> permeability by 76% and 200%, respectively; resulting in 425% enhancement in the capacity of MMM in the sweetening of natural gas with 39.7 selectivity.

#### References

- Ahn, J., Chung, W.-J., Pinnau, I., & Guiver, M. D. (2008). Polysulfone/silica nanoparticle mixed-matrix membranes for gas separation. *Journal of Membrane Science*, 314(1–2), 123-133. doi: <http://dx.doi.org/10.1016/j.memsci.2008.01.031>
- Anadão, P., Sato, L. F., Wiebeck, H., & Valenzuela-Díaz, F. R. (2010). Montmorillonite as a component of polysulfone nanocomposite membranes. *Applied Clay Science*, 48(1–2), 127-132. doi: <http://dx.doi.org/10.1016/j.clay.2009.12.011>
- Ansari, M. O., Yadav, S. K., Cho, J. W., & Mohammad, F. (2013). Thermal stability in terms of DC electrical conductivity retention and the efficacy of mixing technique in the preparation of nanocomposites of graphene/polyaniline over the carbon nanotubes/polyaniline. *Composites Part B: Engineering*, 47, 155-161. doi: <http://dx.doi.org/10.1016/j.compositesb.2012.10.042>
- Aroon, M. A., Ismail, A. F., Matsuura, T., & Montazer-Rahmati, M. M. (2010). Performance studies of mixed matrix membranes for gas separation: A review. *Separation and Purification Technology*, 75(3), 229-242. doi: <http://dx.doi.org/10.1016/j.seppur.2010.08.023>
- Aziz, F., & Ismail, A. F. (2010). Preparation and characterization of cross-linked Matrimid® membranes using para-phenylenediamine for O<sub>2</sub>/N<sub>2</sub> separation. *Separation and Purification Technology*, 73(3), 421-428. doi: <http://dx.doi.org/10.1016/j.seppur.2010.05.002>
- Baker, R. W. (2004). *Gas Separation Membrane Technology and Applications* (pp. 301-353): John Wiley & Sons, Ltd.
- Barrer, R. M., Barrie, J. A., & Rogers, M. G. (1963). Heterogeneous membranes: Diffusion in filled rubber. *Journal of Polymer Science Part A: General Papers*, 1(8), 2565-2586. doi: 10.1002/pol.1963.100010806
- Bertelle, S., Gupta, T., Roizard, D., Vallières, C., & Favre, E. (2006). Study of polymer-carbon mixed matrix membranes for CO<sub>2</sub> separation from flue gas. *Desalination*, 199(1–3), 401-402. doi: <http://dx.doi.org/10.1016/j.desal.2006.03.207>
- Bhide, B. D., Voskericyan, A., & Stern, S. A. (1998). Hybrid processes for the removal of acid gases from natural gas. *Journal of Membrane Science*, 140(1), 27-49. doi: [http://dx.doi.org/10.1016/S0376-7388\(97\)00257-3](http://dx.doi.org/10.1016/S0376-7388(97)00257-3)
- Bhole, Y. S., Wanjale, S. D., Kharul, U. K., & Jog, J. P. (2007). Assessing feasibility of polyarylate-clay nanocomposites towards improvement of gas selectivity. *Journal of Membrane Science*, 306(1–2), 277-286. doi: <http://dx.doi.org/10.1016/j.memsci.2007.09.001>
- Bos, A., Pünt, I., Strathmann, H., & Wessling, M. (2001). Suppression of gas separation membrane plasticization by homogeneous polymer blending. *AIChE Journal*, 47(5), 1088-1093. doi: 10.1002/aic.690470515
- Bos, A., Pünt, I. G. M., Wessling, M., & Strathmann, H. (1998). Plasticization-resistant glassy polyimide membranes

- for CO<sub>2</sub>/CH<sub>4</sub> separations. *Separation and Purification Technology*, 14(1–3), 27-39. doi: [http://dx.doi.org/10.1016/S1383-5866\(98\)00057-4](http://dx.doi.org/10.1016/S1383-5866(98)00057-4)
- Bos, A., Pünt, I. G. M., Wessling, M., & Strathmann, H. (1999). CO<sub>2</sub>-induced plasticization phenomena in glassy polymers. *Journal of Membrane Science*, 155(1), 67-78. doi: [http://dx.doi.org/10.1016/S0376-7388\(98\)00299-3](http://dx.doi.org/10.1016/S0376-7388(98)00299-3)
- Cao, Y., Li, S., Xue, Z., & Guo, D. (1986). Spectroscopic and electrical characterization of some aniline oligomers and polyaniline. *Synthetic Metals*, 16(3), 305-315. doi: [http://dx.doi.org/10.1016/0379-6779\(86\)90167-0](http://dx.doi.org/10.1016/0379-6779(86)90167-0)
- Chung, T.-S., Chan, S. S., Wang, R., Lu, Z., & He, C. (2003). Characterization of permeability and sorption in Matrimid/C<sub>60</sub> mixed matrix membranes. *Journal of Membrane Science*, 211(1), 91-99. doi: [http://dx.doi.org/10.1016/S0376-7388\(02\)00385-X](http://dx.doi.org/10.1016/S0376-7388(02)00385-X)
- Cong, H., Radosz, M., Towler, B. F., & Shen, Y. (2007). Polymer–inorganic nanocomposite membranes for gas separation. *Separation and Purification Technology*, 55(3), 281-291. doi: <http://dx.doi.org/10.1016/j.seppur.2006.12.017>
- Crank, J. (1975). *The mathematics of diffusion*. Oxford Oxford University Press.
- Defontaine, G., Barichard, A., Letaief, S., Feng, C., Matsuura, T., & Detellier, C. (2010). Nanoporous polymer – Clay hybrid membranes for gas separation. *Journal of Colloid and Interface Science*, 343(2), 622-627. doi: <http://dx.doi.org/10.1016/j.jcis.2009.11.048>
- Dong, G., Li, H., & Chen, V. (2011). Plasticization mechanisms and effects of thermal annealing of Matrimid hollow fiber membranes for CO<sub>2</sub> removal. *Journal of Membrane Science*, 369(1–2), 206-220. doi: <http://dx.doi.org/10.1016/j.memsci.2010.11.064>
- Dorosti, F., Omidkhah, M., & Abedini, R. (2014). Fabrication and characterization of Matrimid/MIL-53 mixed matrix membrane for CO<sub>2</sub>/CH<sub>4</sub> separation. *Chemical Engineering Research and Design*, 92(11), 2439-2448. doi: 10.1016/j.cherd.2014.02.018
- Duthie, X., Kentish, S., Powell, C., Nagai, K., Qiao, G., & Stevens, G. (2007). Operating temperature effects on the plasticization of polyimide gas separation membranes. *Journal of Membrane Science*, 294(1–2), 40-49. doi: <http://dx.doi.org/10.1016/j.memsci.2007.02.004>
- Ebadi Amooghin, A., Omidkhah, M., & Kargari, A. (2015). The effects of aminosilane grafting on NaY zeolite–Matrimid@5218 mixed matrix membranes for CO<sub>2</sub>/CH<sub>4</sub> separation. *Journal of Membrane Science*, 490, 364-379. doi: <http://dx.doi.org/10.1016/j.memsci.2015.04.070>
- Ge, L., Zhou, W., Rudolph, V., & Zhu, Z. (2013). Mixed matrix membranes incorporated with size-reduced Cu-BTC for improved gas separation. *JOURNAL OF MATERIALS CHEMISTRY A*, 1, 6350-6358.
- Gh, A. S., & Navarchian, A. H. (2016). Matrimid–polyaniline/clay mixed-matrix membranes with plasticization resistance for separation of CO<sub>2</sub> from natural gas. *Polymers for Advanced Technologies*, 27(9), 1228-1236. doi: 10.1002/pat.3788
- Ghosal, K., & Freeman, B. D. (1994). Gas separation using polymer membranes: an overview. *Polymers for Advanced Technologies*, 5(11), 673-697. doi: 10.1002/pat.1994.220051102
- Gupta, Y., Hellgardt, K., & Wakeman, R. J. (2006). Enhanced permeability of polyaniline based nano-membranes for gas separation. *Journal of Membrane Science*, 282(1–2), 60-70. doi: <http://dx.doi.org/10.1016/j.memsci.2006.05.014>
- Hao, J., Rice, P. A., & Stern, S. A. (2002). Upgrading low-quality natural gas with H<sub>2</sub>S- and CO<sub>2</sub>-selective polymer membranes: Part I. Process design and economics of membrane stages without recycle streams. *Journal of Membrane Science*, 209(1), 177-206. doi: [http://dx.doi.org/10.1016/S0376-7388\(02\)00318-6](http://dx.doi.org/10.1016/S0376-7388(02)00318-6)

- Hashemifard, S. A., Ismail, A. F., & Matsuura, T. (2011). Effects of montmorillonite nano-clay fillers on PEI mixed matrix membrane for CO<sub>2</sub> removal. *Chemical Engineering Journal*, 170(1), 316-325. doi: <http://dx.doi.org/10.1016/j.cej.2011.03.063>
- He, Z., Pinnau, I., & Morisato, A. (2002). Nanostructured poly(4-methyl-2-pentene)/silica hybrid membranes for gas separation. *Desalination*, 146(1-3), 11-15. doi: [http://dx.doi.org/10.1016/S0011-9164\(02\)00463-0](http://dx.doi.org/10.1016/S0011-9164(02)00463-0)
- Hosseini, S. S., Li, Y., Chung, T.-S., & Liu, Y. (2007). Enhanced gas separation performance of nanocomposite membranes using MgO nanoparticles. *Journal of Membrane Science*, 302(1-2), 207-217. doi: <http://dx.doi.org/10.1016/j.memsci.2007.06.062>
- Hosseini, S. S., Peng, N., & Chung, T. S. (2010). Gas separation membranes developed through integration of polymer blending and dual-layer hollow fiber spinning process for hydrogen and natural gas enrichments. *Journal of Membrane Science*, 349(1-2), 156-166. doi: <http://dx.doi.org/10.1016/j.memsci.2009.11.043>
- Hosseini, S. S., Teoh, M. M., & Chung, T. S. (2008). Hydrogen separation and purification in membranes of miscible polymer blends with interpenetration networks. *Polymer*, 49(6), 1594-1603. doi: <http://dx.doi.org/10.1016/j.polymer.2008.01.052>
- Hu, Q., Marand, E., Dhingra, S., Fritsch, D., Wen, J., & Wilkes, G. (1997). Poly(amide-imide)/TiO<sub>2</sub> nanocomposite gas separation membranes: Fabrication and characterization. *Journal of Membrane Science*, 135(1), 65-79. doi: [http://dx.doi.org/10.1016/S0376-7388\(97\)00120-8](http://dx.doi.org/10.1016/S0376-7388(97)00120-8)
- Ismail, A. F., & Lorna, W. (2002). Penetrant-induced plasticization phenomenon in glassy polymers for gas separation membrane. *Separation and Purification Technology*, 27(3), 173-194. doi: [http://dx.doi.org/10.1016/S1383-5866\(01\)00211-8](http://dx.doi.org/10.1016/S1383-5866(01)00211-8)
- Jiang, L. Y., Wang, Y., Chung, T.-S., Qiao, X. Y., & Lai, J.-Y. (2009). Polyimides membranes for pervaporation and biofuels separation. *Progress in Polymer Science*, 34(11), 1135-1160. doi: <http://dx.doi.org/10.1016/j.progpolymsci.2009.06.001>
- Joulazadeh, M., & Navarchian, A. H. (2010). Effect of process variables on mechanical properties of polyurethane/clay nanocomposites. *Polymers for Advanced Technologies*, 21(4), 263-271. doi: 10.1002/pat.1424
- Joulazadeh, M., & Navarchian, A. H. (2011). Study on elastic modulus of crosslinked polyurethane/organoclay nanocomposites. *Polymers for Advanced Technologies*, 22(12), 2022-2031. doi: 10.1002/pat.1713
- Kang, E. T., Neoh, K. G., Tan, T. C., Khor, S. H., & Tan, K. L. (1990). Structural studies of poly(p-phenyleneamine) and its oxidation. *Macromolecules*, 23(11), 2918-2926. doi: 10.1021/ma00213a018
- Kataria, D. (2005). *Polyaniline Clay – Polyimide Hybrid Nanocomposite*. (MASTER OF SCIENCE), B.E. Pune Maharashtra Institute of Technology, Division of Research and Advanced studies of the University of Cincinnati
- Khan, A. L., Klaysom, C., Gahlaut, A., Khan, A. U., & Vankelecom, I. F. J. (2013). Mixed matrix membranes comprising of Matrimid and –SO<sub>3</sub>H functionalized mesoporous MCM-41 for gas separation. *Journal of Membrane Science*, 447, 73-79. doi: <http://dx.doi.org/10.1016/j.memsci.2013.07.011>
- Khan, A. L., Li, X., & Vankelecom, I. F. J. (2011). SPEEK/Matrimid blend membranes for CO<sub>2</sub> separation. *Journal of Membrane Science*, 380(1-2), 55-62. doi: <http://dx.doi.org/10.1016/j.memsci.2011.06.030>
- Koros, W. J., Paul, D. R., & Rocha, A. A. (1976). Carbon dioxide sorption and transport in polycarbonate. *Journal of Polymer Science: Polymer Physics Edition*, 14(4), 687-702. doi: 10.1002/pol.1976.180140410

- Liang, C.-Y., Uchytel, P., Petrychkovych, R., Lai, Y.-C., Friess, K., Sipek, M., . . . Suen, S.-Y. (2012). A comparison on gas separation between PES (polyethersulfone)/MMT (Nanmontmorillonite) and PES/TiO<sub>2</sub> mixed matrix membranes. *Separation and Purification Technology*, 92(0), 57-63. doi: <http://dx.doi.org/10.1016/j.seppur.2012.03.016>
- Lu, H., Hu, Y., Li, M., Chen, Z., & Fan, W. (2006). Structure characteristics and thermal properties of silane-grafted-polyethylene/clay nanocomposite prepared by reactive extrusion. *Composites Science and Technology*, 66(15), 3035-3039. doi: <http://dx.doi.org/10.1016/j.compscitech.2006.01.018>
- Mahajan, R. (2000). *Formation, characterization and modeling of mixed matrix membrane materials*. (PhD), The University of Texas at Austin. (3004329)
- Mahajan, R., Burns, R., Schaeffer, M., & Koros, W. J. (2002). Challenges in forming successful mixed matrix membranes with rigid polymeric materials. *Journal of Applied Polymer Science*, 86(4), 881-890. doi: 10.1002/app.10998
- Matteucci, S., Kusuma, V. A., Kelman, S. D., & Freeman, B. D. (2008). Gas transport properties of MgO filled poly(1-trimethylsilyl-1-propyne) nanocomposites. *Polymer*, 49(6), 1659-1675. doi: <http://dx.doi.org/10.1016/j.polymer.2008.01.004>
- Matteucci, S., Kusuma, V. A., Sanders, D., Swinnea, S., & Freeman, B. D. (2008). Gas transport in TiO<sub>2</sub> nanoparticle-filled poly(1-trimethylsilyl-1-propyne). *Journal of Membrane Science*, 307(2), 196-217. doi: <http://dx.doi.org/10.1016/j.memsci.2007.09.035>
- Matteucci, S., Kusuma, V. A., Swinnea, S., & Freeman, B. D. (2008). Gas permeability, solubility and diffusivity in 1,2-polybutadiene containing brookite nanoparticles. *Polymer*, 49(3), 757-773. doi: <http://dx.doi.org/10.1016/j.polymer.2007.12.011>
- Matteucci, S., Raharjo, R. D., Kusuma, V. A., Swinnea, S., & Freeman, B. D. (2008). Gas Permeability, Solubility, and Diffusion Coefficients in 1,2-Polybutadiene Containing Magnesium Oxide. *Macromolecules*, 41(6), 2144-2156. doi: 10.1021/ma702459k
- Mekhmer, G. A. H., Halawy, S. A., Mohamed, M. A., & Zaki, M. I. (2004). Qualitative and Quantitative Assessments of Acid and Base Sites Exposed on Polycrystalline MgO Surfaces: Thermogravimetric, Calorimetric, and in-Situ FTIR Spectroscopic Study Combination. *The Journal of Physical Chemistry B*, 108(35), 13379-13386. doi: 10.1021/jp040164s
- Moaddeb, M., & Koros, W. J. (1997). Gas transport properties of thin polymeric membranes in the presence of silicon dioxide particles. *Journal of Membrane Science*, 125(1), 143-163. doi: [http://dx.doi.org/10.1016/S0376-7388\(96\)00251-7](http://dx.doi.org/10.1016/S0376-7388(96)00251-7)
- Moghadam, F., Omidkhah, M. R., Vasheghani-Farahani, E., Pedram, M. Z., & Dorosti, F. (2011). The effect of TiO<sub>2</sub> nanoparticles on gas transport properties of Matrimid5218-based mixed matrix membranes. *Separation and Purification Technology*, 77(1), 128-136. doi: <http://dx.doi.org/10.1016/j.seppur.2010.11.032>
- Moore, T. T., & Koros, W. J. (2005). Non-ideal effects in organic-inorganic materials for gas separation membranes. *Journal of Molecular Structure*, 739(1-3), 87-98. doi: <http://dx.doi.org/10.1016/j.molstruc.2004.05.043>
- Narayanan, B. N., Koodathil, R., Gangadharan, T., Yaakob, Z., Saidu, F. K., & Chandralayam, S. (2010). Preparation and characterization of exfoliated polyaniline/montmorillonite nanocomposites. *Materials Science and Engineering: B*, 168(1-3), 242-244. doi: <http://dx.doi.org/10.1016/j.mseb.2009.12.027>
- Noble, R. D. (2011). Perspectives on mixed matrix membranes. *Journal of Membrane Science*, 378(1-2), 393-397. doi: <http://dx.doi.org/10.1016/j.memsci.2011.05.031>

- Pacchioni, G. (1993). Physisorbed and chemisorbed CO<sub>2</sub> at surface and step sites of the MgO(100) surface. *Surface Science*, 281(1–2), 207-219. doi: [http://dx.doi.org/10.1016/0039-6028\(93\)90869-L](http://dx.doi.org/10.1016/0039-6028(93)90869-L)
- Paul, D. R. (1979). Gas Sorption and Transport in Glassy Polymers. *Berichte der Bunsengesellschaft für physikalische Chemie*, 83(4), 294-302. doi: 10.1002/bbpc.19790830403
- Pavia, D. L., Lampman, G. M., Kriz, G. S., & Vyvyan, J. A. (2015). *Introduction to Spectroscopy*: Cengage Learning.
- Perez, E. V., Balkus Jr, K. J., Ferraris, J. P., & Musselman, I. H. (2014). Metal-organic polyhedra 18 mixed-matrix membranes for gas separation. *Journal of Membrane Science*, 463, 82-93. doi: <http://dx.doi.org/10.1016/j.memsci.2014.03.045>
- Ploegmakers, J., Japip, S., & Nijmeijer, K. (2013). Mixed matrix membranes containing MOFs for ethylene/ethane separation—Part B: Effect of Cu<sub>3</sub>BTC<sub>2</sub> on membrane transport properties. *Journal of Membrane Science*, 428, 331-340. doi: <http://dx.doi.org/10.1016/j.memsci.2012.11.013>
- Rebattet, L., Escoubes, M., Pinéri, M., & Geniès, E. M. (1995). Proceedings of the International Conference on Science and Technology of Synthetic Metals (ICSM '94) Gas sorption in polyaniline powders and gas permeation in polyaniline films. *Synthetic Metals*, 71(1), 2133-2137. doi: [http://dx.doi.org/10.1016/0379-6779\(94\)03197-E](http://dx.doi.org/10.1016/0379-6779(94)03197-E)
- Robeson, L. M. (2008). The upper bound revisited. *Journal of Membrane Science*, 320(1–2), 390-400. doi: <http://dx.doi.org/10.1016/j.memsci.2008.04.030>
- Scholes, C. A., Stevens, G. W., & Kentish, S. E. (2012). Membrane gas separation applications in natural gas processing. *Fuel*, 96(0), 15-28. doi: <http://dx.doi.org/10.1016/j.fuel.2011.12.074>
- Scholes, C. A., Tao, W. X., Stevens, G. W., & Kentish, S. E. (2010). Sorption of methane, nitrogen, carbon dioxide, and water in Matrimid 5218. *Journal of Applied Polymer Science*, 117(4), 2284-2289.
- Shahid, S., & Nijmeijer, K. (2014a). High pressure gas separation performance of mixed-matrix polymer membranes containing mesoporous Fe(BTC). *Journal of Membrane Science*, 459(0), 33-44. doi: <http://dx.doi.org/10.1016/j.memsci.2014.02.009>
- Shahid, S., & Nijmeijer, K. (2014b). Performance and plasticization behavior of polymer–MOF membranes for gas separation at elevated pressures. *Journal of Membrane Science*, 470, 166-177. doi: <http://dx.doi.org/10.1016/j.memsci.2014.07.034>
- Shi, X., & Gan, Z. (2007). Preparation and characterization of poly(propylene carbonate)/montmorillonite nanocomposites by solution intercalation. *European Polymer Journal*, 43(12), 4852-4858. doi: <http://dx.doi.org/10.1016/j.eurpolymj.2007.09.024>
- Sridhar, S., Veerapur, R. S., Patil, M. B., Gudasi, K. B., & Aminabhavi, T. M. (2007). Matrimid polyimide membranes for the separation of carbon dioxide from methane. *Journal of Applied Polymer Science*, 106(3), 1585-1594. doi: 10.1002/app.26306
- Su, T. M., Ball, I. J., Conklin, J. A., Huang, S.-C., Larson, R. K., Nguyen, S. L., . . . Kaner, R. B. (1997). Polyaniline/polyimide blends for pervaporation and gas separation studies. *Synthetic Metals*, 84(1–3), 801-802. doi: [http://dx.doi.org/10.1016/S0379-6779\(96\)04153-7](http://dx.doi.org/10.1016/S0379-6779(96)04153-7)
- Tang, J., Jing, X., Wang, B., & Wang, F. (1988). Infrared spectra of soluble polyaniline. *Synthetic Metals*, 24(3), 231-238. doi: [http://dx.doi.org/10.1016/0379-6779\(88\)90261-5](http://dx.doi.org/10.1016/0379-6779(88)90261-5)
- Taveira, P., Mendes, A., & Costa, C. (2003). On the determination of diffusivity and sorption coefficients using different time-lag models. *Journal of Membrane Science*, 221(1–2), 123-133. doi: [http://dx.doi.org/10.1016/S0376-7388\(03\)00252-7](http://dx.doi.org/10.1016/S0376-7388(03)00252-7)

- Taylor, J. R. (1997). *An Introduction to Error Analysis: The Study of Uncertainties in Physical Measurements*. Sausalito, CA: University Science Books.
- Tena, A., Fernández, L., Sánchez, M., Palacio, L., Lozano, A. E., Hernández, A., & Prádanos, P. (2010). Mixed matrix membranes of 6FDA-6FpDA with surface functionalized  $\gamma$ -alumina particles. An analysis of the improvement of permselectivity for several gas pairs. *Chemical Engineering Science*, 65(6), 2227-2235. doi: <http://dx.doi.org/10.1016/j.ces.2009.12.023>
- Tin, P. S., Chung, T. S., Liu, Y., Wang, R., Liu, S. L., & Pramoda, K. P. (2003). Effects of cross-linking modification on gas separation performance of Matrimid membranes. *Journal of Membrane Science*, 225(1-2), 77-90. doi: <http://dx.doi.org/10.1016/j.memsci.2003.08.005>
- Wind, J. D., Staudt-Bickel, C., Paul, D. R., & Koros, W. J. (2002). The Effects of Crosslinking Chemistry on CO<sub>2</sub> Plasticization of Polyimide Gas Separation Membranes. *Industrial & Engineering Chemistry Research*, 41(24), 6139-6148. doi: 10.1021/ie0204639
- Xiao, Y., Low, B. T., Hosseini, S. S., Chung, T. S., & Paul, D. R. (2009). The strategies of molecular architecture and modification of polyimide-based membranes for CO<sub>2</sub> removal from natural gas—A review. *Progress in Polymer Science*, 34(6), 561-580. doi: <http://dx.doi.org/10.1016/j.progpolymsci.2008.12.004>
- Yampolskii, Y., Pinnau, I., & Freeman, B. (2006). *Materials Science of Membranes for Gas and Vapor Separation*. John Wiley & Sons Ltd, The Atrium, Southern Gate, Chichester, West Sussex PO19 8SQ, England: John Wiley & Sons Ltd.
- Zhang, L., Xiao, Y., Chung, T.-S., & Jiang, J. (2010). Mechanistic understanding of CO<sub>2</sub>-induced plasticization of a polyimide membrane: A combination of experiment and simulation study. *Polymer*, 51(19), 4439-4447. doi: <http://dx.doi.org/10.1016/j.polymer.2010.07.032>
- Zhang, Y., Balkus Jr, K. J., Musselman, I. H., & Ferraris, J. P. (2008). Mixed-matrix membranes composed of Matrimid® and mesoporous ZSM-5 nanoparticles. *Journal of Membrane Science*, 325(1), 28-39. doi: <http://dx.doi.org/10.1016/j.memsci.2008.04.063>
- Zhao, H.-Y., Cao, Y.-M., Ding, X.-L., Zhou, M.-Q., Liu, J.-H., & Yuan, Q. (2008). Poly(ethylene oxide) induced cross-linking modification of Matrimid membranes for selective separation of CO<sub>2</sub>. *Journal of Membrane Science*, 320(1-2), 179-184. doi: <http://dx.doi.org/10.1016/j.memsci.2008.03.070>

#### Abbreviations:

DSC: Differential Scanning Calorimetry

FESEM: Field Emission Scanning Electron Microscopy

FTIR-ATR: Fourier Transform Infrared equipped with Attenuated Total Reflection

MMM: Mixed-Matrix Membrane

NMP: N-methyl-2-pyrrolidone

PAni: Polyaniline, PC: Polyaniline/Clay

$p_{plast}$ : Plasticization Pressure

TGA: Thermogravimetric Analysis

XRD: X-ray Diffraction